Research on Chemical Intermediates (2023) 49:701–716
https://doi.org/10.1007/s11164-022-04897-1

Aminated polyacrylonitrile fibers for the removal of hydrogen sulfide from natural gas at room temperature

Zhihao Liu[1] · Kui Qiu[1] · Gang Sun[2] · Yue Ma[2] · Yingjie Wang[1] · Jianghu Peng[1] · Song Chen[1] · Xiaochuan Song[1]

Received: 30 August 2022 / Accepted: 25 November 2022 / Published online: 4 December 2022

Abstract

H_2S is a common toxic gas in natural gas processing, and adsorption is a promising technology for hydrogen sulfide removal. However, current desulfurization agents suitable for low ambient temperatures and easy regeneration remain a challenge. In this paper, aminated polyacrylonitrile was directly synthesized in a one-step reaction from widely available engineering PANF (polyacrylonitrile fiber) for H_2S removal at ambient temperature. The fiber samples at various stages were characterized in detail, and the adsorption behavior of PANF-DETA (diethylenetriamine) on H_2S under different conditions (weight gain rate, temperature, moisture) was investigated. The results showed that the aminated fibers could rapidly absorb H_2S by acid–base proton reaction. The optimal sulfur capacity of H_2S reached 16.2 mg/g when the weight increase rate of aminated fibers was 60%, which was 15 times greater than the adsorption capacity of pure polyacrylonitrile fibers. The saturated fiber can be effectively regenerated through alkali rinsing. After ten consecutive regenerations, the sulfur capacity of the aminated fiber is 13.6 mg/g, which remains at more than 80% of the initial capacity. Overall, fiber sorbents have excellent thermal stability, reusability, chemical stability. It can effectively adapt to various practical application environments and is a promising new type of adsorbent.

Keywords PANF · Amination reaction · Ambient desulfurization agent · Regeneration performance

✉ Kui Qiu
2020205053@cqust.edu.cn

[1] School of Chemistry and Chemical Engineering, Chongqing University of Science and Technology, No.20 Daxuecheng East Road, Shapingba District, Chongqing 401331, China

[2] Northwest Sichuan Gas Mine of Southwest Oil Field, Southwest Oil and Gas Field Company, PetroChina, Jiangyou 621709, Sichuan, China

Introduction

The presence of hydrogen sulfide, a common contaminant in natural gas processing, poses a significant threat to human health and causes catalyst poisoning, equipment pipe corrosion, and severe environmental contamination (e.g., acid rain) through sulfur dioxide generation [1–3]. In order to ensure the safety of natural gas production and use, it must be strictly removed. Over the years, scientists and researchers have developed a variety of H_2S treatment technologies for complex desulfurization scenarios, including catalytic oxidation desulfurization [4], adsorption [5], wet absorption [6], and selective oxidation [7]. Generally, natural gas with a hydrogen sulfide concentration of less than 2% (mol/%) or daily sulfur content of less than 5t/d is referred to as a medium to a low sulfur-bearing gas reservoir [8]. Adsorption is widely used to remove hydrogen sulfide from small- and medium-scale sulfur-bearing gas reservoirs because of its mild operating conditions, high degree of purification, energy, and cost savings. However, as the most extensively used commercial adsorbents, metal oxide-based adsorbents are limited by reaction kinetics and can only show strong H_2S purification capability in harsh medium to high-temperature conditions [9–12]. In addition, most of these used adsorbents are currently disposed of in the form of discard or landfill, which cannot achieve the effect of resource utilization and causes severe ecological pollution [13]. In order to avoid these problems, researchers are developing new strategies to provide more effective solutions.

In recent years, many new porous adsorbents such as activated carbon [14], graphene oxide [15], zeolite [16], mesoporous silica [17], and metal–organic frameworks (MOFs) [18] materials have been used for the removal of H_2S from natural gas at room temperature and have demonstrated impressive performance. However, high preparation costs, complex preparation process, structural instability, and low reproducibility limit their further application in gas purification [19]. In general, enhancing the regeneration capability of sorbents is crucial because the majority of sorbents currently utilized cannot be recycled and may even need to be disposed of in landfills [20]. The carrier is a crucial factor affecting the lifetime of the adsorbent. As an essential component of solid adsorbents, there are generally strict requirements for their use. Developing green, stable, efficient, and universally applicable carriers have been one of the main focuses of adsorbent material design. As one of the three primary synthetic fibers used today, PANF (Polyacrylonitrile fiber) has a high specific surface area, is rich in cyano, and is chemically active, allowing it to be easily chemically modified and converted into functionalized fibers with other functional groups [21]. Protected by polymer chains, PANF also has excellent chemical resistance, high thermal stability, and good mechanical properties [22]. In addition, as a very mature man-made fiber, in the actual desulfurization scenario, people can use it according to the process requirements for its directional mechanical processing into suitable shapes (such as filament bundles, woolen strips, non-woven fabrics, fiber columns), which provides even more advantages for its use as a substrate material for desulfurization agents [23]. More importantly, unlike metal oxide-based adsorbents, PANF

with a carbon chain backbone has the advantage of being naturally environmentally friendly. Currently, polyacrylonitrile materials have been widely used in the removal, separation enrichment, detection, and catalytic preparation of heavy metal ions and organic dyes [24]. To the best of our knowledge, there are few studies on applying polyacrylonitrile fibers to acid gas adsorption. Most studies on using fibrous materials for H_2S capture have focused on improving the adsorption performance, neglecting the critical reusability for its practical application [25–27].

Amine groups are one of the basic adsorption groups that exhibit a high binding ability to many acidic groups. In the field of hydrogen sulfide removal, the widely used alcohol-amine method [28] utilizes the acid–base interaction between amine groups and hydrogen sulfide to achieve hydrogen sulfide uptake. In designing various solid adsorbents, researchers often graft amine groups onto the surface of the carrier to effectively improve the desulfurization efficiency. Since cyano (–CN) does not directly interact with H_2S, the physical adsorption of H_2S by PANF's pore structure alone cannot achieve the purification standard. Herein, we prepared aminated polyacrylonitrile fibers ($PANF_{DETA}$) by a one-step reaction using commercially available polyacrylonitrile fibers as the base material and DETA as the modifying reagent to use them for hydrogen sulfide removal at room temperature. Desulfurization experiments investigated the adsorption behavior of fibers on H_2S, and the focus was on the excellent regeneration performance of the fiber adsorbent to evaluate its potential as a desulfurizer substrate material. The fiber samples at various stages were systematically characterized by Fourier transform infrared spectroscopy (FTIR), thermogravimetric analyzer (TGA), swept surface electron microscopy (SEM), and X-ray diffractometer (XRD), aiming to provide new ideas for the removal of H_2S at room temperature.

Experimental

Materials and reagents

Polyacrylonitrile fiber (commercially available), diethylenetriamine, ethanol, hydrochloric acid, sodium hydroxide, acetic acid, and zinc chloride, analytically pure, were all purchased from Chengdu Kelong Chemical Reagent Factory.

Apparatus and instruments

The modifications of the functional groups on the surface of the fibers were observed by using a Fourier transform infrared spectrometer (FT-IR, KBr, 4000-500 cm1) BRUKE TENS OR27 (Germany). The thermal stability of the fibers was tested in a nitrogen atmosphere from room temperature to 800 °C at a rate of 10 °C min^{-1} using a TG/DTA 6300 simultaneous thermal analyzer (Netzsch Company, Germany). To track the changes in the elemental composition of the fibers, a Vario EL Cube elemental analyzer (Germany) was used (C, N, and O). Using a Japanese

XD series X-ray diffractometer (CuK radiation at 40 kV and 30 mA), fibers with different interior crystal structures were highlighted. A PHS-3E pH meter (Shanghai Yidian Scientific Instrument Co., China) measured the solution pH. The sample was dispersed uniformly on a conductive adhesive tape, which was bonded to the sample holder, and the excess sample was blown off using an ear wash ball. A Zeiss sigma300 observed the surface morphology of the fibers at different stages and swept the surface electron microscope.

Preparation of fiber adsorbent

The specific preparation steps of aminated fibers are as follows: Firstly, PANF is torn into fine filaments and placed in ethanol for 6–8 h to wash away possible impurities on the fiber surface. The fibers are removed, washed with distilled water to neutral, dried at 50 °C to constant weight, and sealed for storage. In order to prevent cyanohydrolysis and the generation of amide structures, a pure amine solution was chosen as the reaction solvent. Take 10 g of pretreated PANF submerged in anhydrous diethylenetriamine (analytical purity), raise the temperature to 125–130℃, continuous reflux stirring for 4–6 h and observe the fiber state, stop the reaction when the fiber starts to melt. After the reaction was completed, to thoroughly clean the organic amine residue on the fiber surface, the fibers were removed after the flask was cooled entirely and rinsed repeatedly with hot water at 70–80 °C until the filtrate pH was 7–8. Next, the fibers were rinsed with distilled water and anhydrous ethanol until the pH was stabilized at pH 7. Finally, the fibers were dried at 50 °C to a constant weight and weighed to obtain golden yellow aminated fibers. The reaction schematic of the preparation process is shown in Fig. 1.As an important indicator to

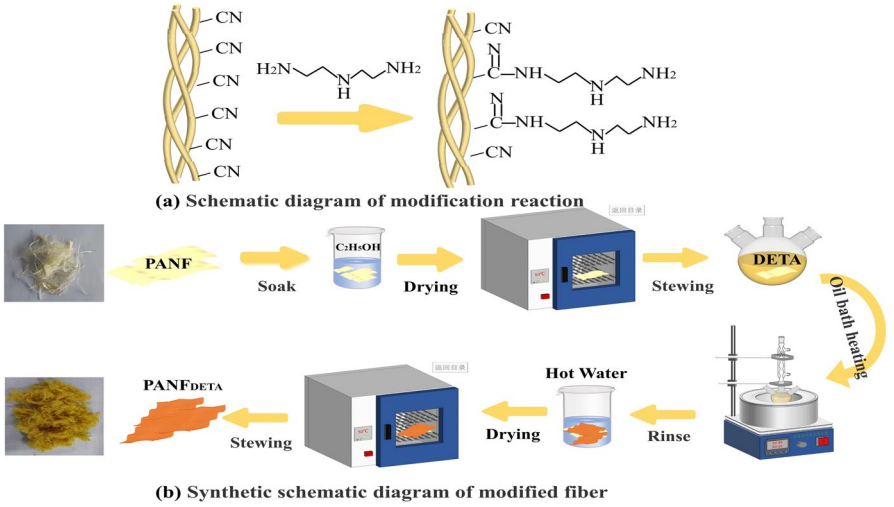

Fig.1 Preparation of aminated fiber adsorbent: **a** schematic diagram of modification reaction; **b** synthetic schematic diagram of modified fiber

evaluate the degree of amination reaction, the rate of fiber weight gain is determined by the Eq. (1):

$$W = \frac{m_2 - m_1}{m_1} \times 100\% \tag{1}$$

W is the weight gain rate (%); m_1 and m_2 are the masses (g) of fibers before and after the reaction.

Desulfurization and regeneration experiments

The adsorption experiments were performed in a fixed-bed metal reactor (height 8 cm, diameter 6 mm). Stainless steel columns were used as fixed beds for H_2S adsorption to achieve smooth and well-dispersed adsorbent. The sulfur-containing gas used was a standard gas with a mass concentration of 5300 ppm. The gas flow rate used for the experiments was 5 ml/min, controlled by a mass flow meter. The fiber dosage was 0.5 g. This gas was passed into the metal tube containing the adsorbent for the desulfurization experiments. The room temperature was 40 °C. The composition of the effluent gas was analyzed with a gas analyzer (Methanex, Inc., USA) with a detection limit of 0.1 ppm. The H_2S concentration in the exhaust gas is measured every 5 min until the H_2S concentration in the outflow gas reaches 4 ppm; then, the experiment is stopped, and the corresponding time is recorded as the penetration time.

Prepare 50 ml of different concentrations of sodium hydroxide solution for the desorption of saturated fibers. After the desulfurization experiment, the fibers were taken out and immersed in sodium hydroxide solutions with different concentrations for a predetermined time and then taken out and repeatedly washed with distilled water and anhydrous ethanol until the pH of the eluent was between 7 and 8. Finally, the fibers were dried to a constant weight at 60–80 °C for the next desulfurization experiment. This process is considered a complete regeneration process.

In order to better evaluate the regeneration performance of $PANF_{DETA}$, we used the desorption rate to evaluate the degree of regeneration of the aminated fibers. Considering the presence of HS- in saturated fibers and the fact that the sulfur ion content in the solution cannot be detected by conventional titration means under alkaline conditions. To avoid the volatilization of HS^- to H_2S under strongly acidic conditions, we first neutralized the remaining NaOH by adding acetic acid to the lye, adjusted the pH to about 5, and titrated the content of S^{2-} in the regenerated lye by adding $ZnCl_2$ dropwise. The amount of $ZnCl_2$ consumed equals the actual S^{2-} in the solution. After elution, the fibers were rinsed with deionized water and anhydrous ethanol to thoroughly wash the remaining alkali on the fiber surface and dried under vacuum at 60 °C for 2 h. Dry the fiber and remove it for subsequent use. The desorption rate is calculated according to Eq. (2):

$$D = \frac{n_0}{n_1} \times 100\% \tag{2}$$

where n_1 is the amount of H_2S adsorbed on the fiber and n_0 is the amount of S^{2-} obtained by titration in the eluent after desorption.

Result and discussion

Characterization results of PANF

FTIR spectroscopy

Figure 2 shows the infrared spectra of the fibers before and after the modification reaction. Compared to the original fiber, the broad peak area at 3700–3150 cm^{-1} of the aminated fiber is significantly larger, corresponding to the N–H stretch at the amide bond generated by the reaction between the primary amine group and the cyano group in DETA [29]. The intensity of the absorption peak at 2240 cm^{-1} of the aminated fiber can be observed to be significantly reduced due to the consumption of the cyano group in the reaction but still maintains a certain intensity, indicating that only part of the cyano group is involved in the reaction. Due to the multi-amine structure of DETA, the broad peaks at 1297 cm^{-1} and 1553 cm^{-1} of the aminated fibers correspond to the N–H bending peaks in the amine group and the N–H bending interactions in C–N–H, respectively [30]. In addition, it is not difficult to find an increase in the peak area of the C–N stretching peak at 1456 cm^{-1} before and after the reaction, which proves the introduction of the carbon chain in DETA [31]. These results indicate that DETA was successfully grafted onto the PANF substrate through the amination reaction with –CN.

Elements analysis

The results of elemental fiber analysis at each stage are shown in Table 1. The carbon content of $PANF_{DETA}$ is significantly lower, and the hydrogen content is higher than the original fiber. This is caused by the fact that the carbon content of the

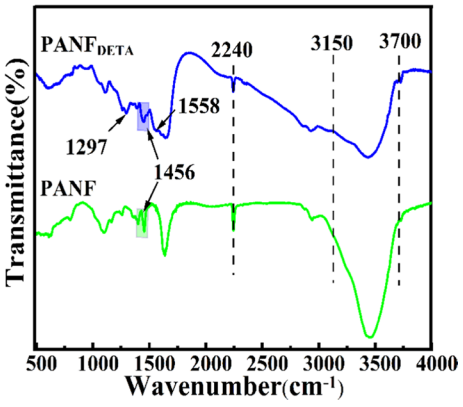

Fig. 2 The FTIR spectra of PANF and $PANF_{DETA}$

Table 1 Fiber weight gain rate and elemental content at each stage

Fiber sample	*N*(%)	*C*(%)	*H*(%)
PANF	25.45	66.06	5.31
$PANF_{DETA}$	19.07	43.01	6.72
$PANF_{DETA}$-1	18.09	45.13	7.24
$PANF_{DETA}$-10	16.14	44.47	7.51

DETA portion of the fiber graft is lower than that of PANF, while the hydrogen content is higher than that of PANF. In addition, the significant decrease in nitrogen content also indicates that the modification reaction was accompanied by a cross-linking reaction of polyacrylonitrile, which suggests that PANF did undergo the expected chemical reaction with DETA and successfully introduced amines to some extent [32]. It is noteworthy that the C, H, and N contents of $PANF_{DETA}$-1 and $PANF_{DETA}$-10 are essentially the same as those of $PANF_{DETA}$. The slight decrease in N and C contents may be due to the shedding of a small number of amine groups during the desulfurization–regeneration process and the adhesion of unwashed NaOH molecules to the fiber surface. The decrease of N content is less than 3% compared with fresh fibers after ten times of use, indicating that $PANF_{DETA}$ is structurally stable. Overall, the elemental analysis results indicate that $PANF_{DETA}$ is structurally stable and has good reusability.

X-ray diffraction spectroscopy (XRD) analysis

In polyacrylonitrile fibers, polymer chains are tightly clustered in an irregular helical conformation. Although there is no strict crystalline region, the highly ordered arrangement of polyacrylonitrile molecules allows acrylic fibers to maintain high stability and mechanical strength [33]. This structural feature is reflected in the X-ray powder diffraction pattern by the presence of distinct spikes at 2θ angles of 17°, 29.5°, and 37.75° [34]. As seen in Fig. 3, the intensity of the characteristic diffraction peaks of the aminated acrylic fibers decreased significantly,

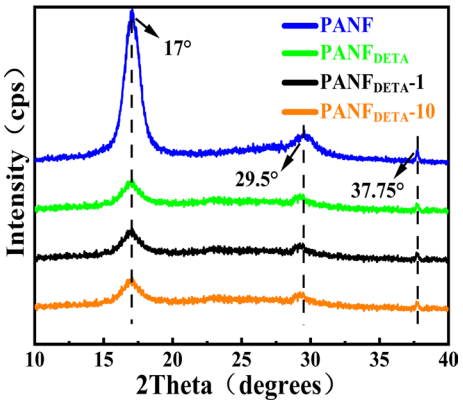

Fig.3 The XRD patterns of PANF, $PANF_{DETA}$, $PANF_{DETA}$-1, $PANF_{DETA}$-10

which indicates that the high-order arrangement of polyacrylonitrile underwent a certain degree of dissolution and destruction by DETA, but still maintained a specific strength. The XRD patterns of the fibers after desulfurization and regeneration after 1 time and 10 times were not significantly different from those of the aminated fibers, which proved that the high-order arrangement of the fibers was not further destroyed during the subsequent desulfurization and regeneration process [35]. The fibers still maintained good mechanical properties, which is significant in the practical application of the fibers.

Scanning electron microscope (SEM)

The surface morphology of the original, modified, and after-desulfurized fibers under the scanning electron microscope is shown in Fig. 4, respectively. There was no significant change in the surface of the fibers before and after the reaction. The images of $PANF_{DETA}$ fibers obtained at 1000 × and 5000 × magnification show a smooth surface with almost no cracks, indicating that the modified fibers can maintain good stability. Due to the chemical grafting reaction and the expansion of the fibers, the diameter of $PANF_{DETA}$ increased significantly compared to the original fibers. The fiber diameter increases the contact area between the fiber and the adsorbent, which facilitates adsorption [36]. Fine particles cover the

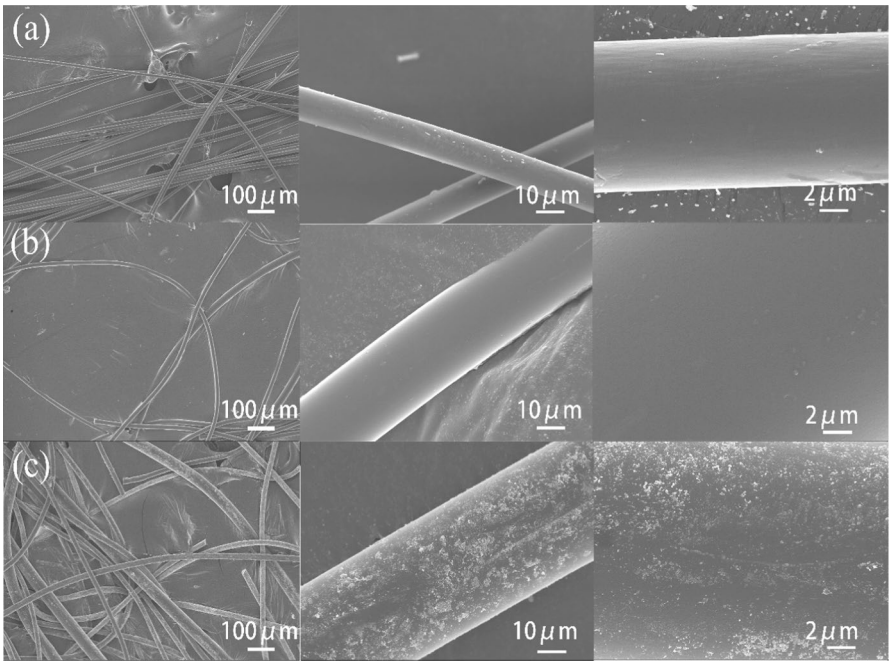

Fig. 4 The SEM images of **a** PANF, **b** PANAF, and **c** PANAF-H_2S magnifications are 100, 1000, and 5000 times

fiber's surface after desulfurization due to the interaction with hydrogen sulfide. However, it can be observed that the fiber surface remains flat without apparent damage, indicating that the overall structure is well maintained.

Thermogravimetric analysis

Thermogravimetric spectra were used to study the thermal stability of the fibers. Thermogravimetric spectra were recorded from 30 °C to 800 °C at a heating rate of 10 °C per minute under a nitrogen atmosphere. The results are shown in Fig. 5. The original PANF showed almost no mass loss at 300 °C. When the temperature reached 800 °C, the remaining mass was still more than 50%, showing its high thermal stability. As for the functionalized fibers, $PANF_{DETA}$ shows substantial mass loss phases in the temperature range of 100–450 °C, which can be attributed to the evaporation of moisture and volatile residues, the decomposition of the modified groups on the fiber surface, and the gradual destruction of the polyacrylonitrile fiber backbone, respectively [37]. Compared with the original PANF, the thermal stability of $PANF_{DETA}$ decreases significantly. Therefore, in practical applications, the use temperature should be kept within 100 °C to maintain the stability of the active components on the fiber surface and the backbone structure [38].

Desulfurization performance study of adsorbent

Effect of different weight gain rates on desulfurization performance

The higher weight gain rate means more amino groups are grafted on the fiber surface. The introduction of amino groups can provide an active site for H_2S molecules and promote the diffusion of H_2S molecules inside the fibers [39]. Figure 6a and b shows the H_2S breakthrough curves measured on fibers with different weight gain rates and corresponding sulfur capacity distributions, respectively. For comparison, we also measured the H_2S breakthrough curves on unmodified PANF. Figure 6a shows that the unmodified PANF sample has the quickest breakthrough time and

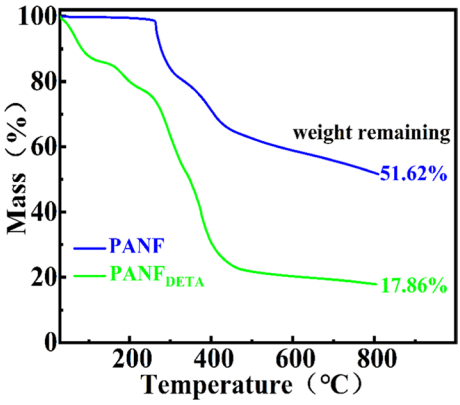

Fig.5 The TGA spectra of PANF and $PANF_{DETA}$

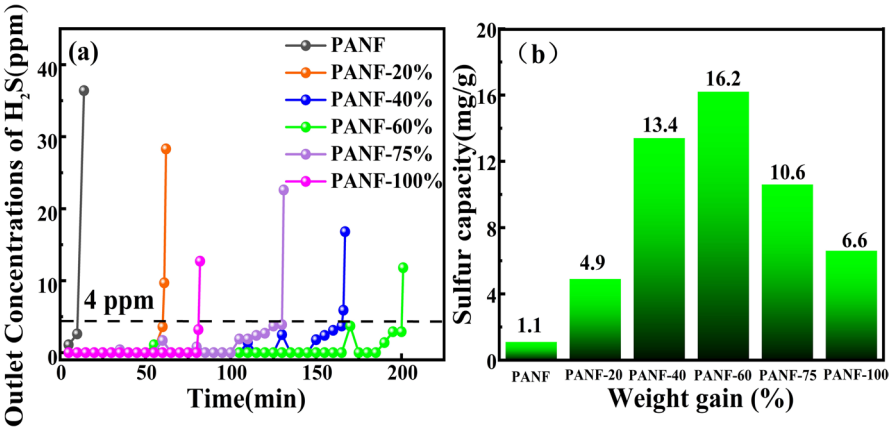

Fig.6 **a** Breakthrough curves for fibers with different weight gain rates (T = 40°C, H_2S feed gas = 5300 ppm, N_2 balance, gas flow = 5 ml/min). **b** Sulfur capacity corresponds to fibers with different weight gain rates

the least H_2S removal capacity, corresponding to an H_2S breakthrough capacity of just 1.1 mg/g (Fig. 6b). The H_2S removal capacity of the amination-modified fibers increased significantly. It showed a volcano-like trend with an increasing weight gain rate. The fiber sample with a 60% weight gain rate had the highest H_2S breakthrough capacity of 16.2 mg/g. Notably, the adsorption capacity of the fiber for H2S decreased as the weight gain rate continued to increase. This may be due to the continuation of the amination reaction destroying the fiber skeleton structure and collapsing the internal pore structure. This not only limits the diffusion of H_2S molecules inside the fiber but also reduces the mechanical strength of the fiber. In addition, it is evident from the breakthrough curves that the fiber samples with different weight gain rates exhibit similar adsorption behavior. They can all adsorb H_2S efficiently at the initial stage to maintain their H_2S concentration at the tail gas to meet the purification index, and then breakthrough occurs rapidly, which implies fast reaction kinetics of H_2S adsorption by the fibers [40].

Effect of different temperatures on desulfurization performance

The reaction temperature influences the adsorption of gas molecules on the catalyst surface and the chemical reaction. At lower temperatures, the outside world cannot provide enough activation energy for the chemical reaction to proceed effectively, and the chemisorption effect is poor. Too high a temperature generates a lot of energy consumption and wastes resources [41]. The effect of temperature on the performance of fiber adsorbent desulfurization is shown in Fig. 7. With increasing temperature, the corresponding permeation time increases slightly, suggesting that the increase in temperature facilitates this adsorption process. At 20 °C, the fibers have the lowest purification time of 175 min. At 50 °C, this value reaches a maximum of 201 min. Increasing the reaction temperature enhances the mass transfer and increases the chemical reaction rate, which is more favorable for the rapid binding

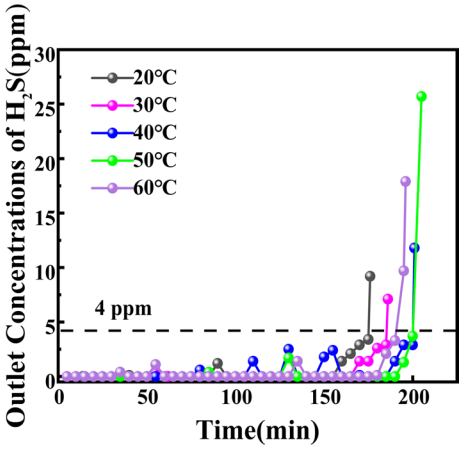

Fig.7 Breakthrough curves for fibers with different temperatures. (H_2S feed gas = 5300 ppm, N_2 balance, gas flow = 5 ml/min)

of H_2S to the functional groups on the fiber surface. Temperature increase can promote the chemisorption process but not the physical adsorption process, which, to some extent, also indicates that the adsorption of H_2S by fibers is mainly chemisorption [37]. Continuing to increase the temperature, the fibers' purification capacity decreased at 60 °C. This may be because the increase in reaction rate reduces the time that H_2S molecules can effectively contact the surface-active sites, leading to a decrease in fiber purification capacity. Since the fibers exhibited a breakthrough time of 201 min at both 40 °C and 50 °C, 40 °C was considered the optimal reaction temperature considering energy saving and milder reaction conditions.

Effect of moisture on desulfurization performance

Since the aminated fibers have good water absorption and some moisture is inevitably and commonly incorporated in the actual industrial gas stream, it is necessary to study the effect of moisture on H_2S removal [42]. Figure 8 compares breakthrough

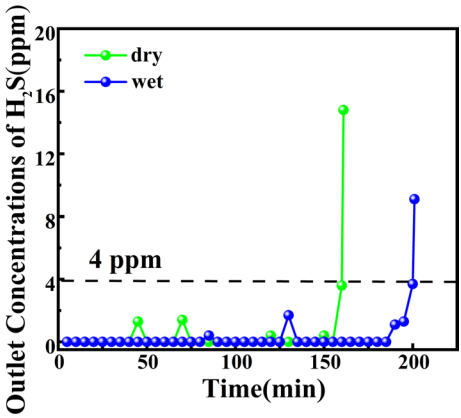

Fig.8 Breakthrough curves for fibers with different Moisture content. (T = 40.°C, H_2S feed gas = 5300 ppm, N_2 balance, gas flow = 5 ml/min)

curves of wet and dry fibers under an H_2S gas mixture. The figure shows that the breakthrough time for H_2S in dry gas is 160 min. In the presence of moisture, the corresponding breakthrough time for the fiber adsorbent under wetting is 201 min. This is mainly because the reaction between H_2S and the active sites on the fiber surface is a gas–solid reaction, and it is difficult for the two to contact and interact with each other fully. The moisture entry can form a water film on the fiber surface, which directly enhances the gas–solid mass transfer and promotes the ionization of H_2S into HS^-. It has been shown that the affinity between the charged HS^- and the active site is more potent than between the gaseous H_2S. On the other hand, water can promote the swelling of fibers, which makes H_2S molecules diffuse quickly into the fibers, and this also promotes the adsorption of H_2S[43].

Regeneration performance study of adsorbent

Effect of sodium hydroxide concentration and soaking time on regeneration performance

During the regeneration process, the H_2S molecules adsorbed on the fibers are eluted by reacting with sodium hydroxide to form Na_2S or NaHS. Theoretically, the grafted amino groups on the fiber surface will be restored to their initial state, restoring the sulfur capacity. However, in actual use, the grafted amino groups on the fiber surface may fall off, decreasing desulfurization performance. On the other hand, since polyacrylonitrile fibers are not resistant to an alkaline environment, improper control in an alkaline environment, such as too high a concentration of alkali and too long contact time, will cause damage to the –CN functional group structure on the fiber backbone[44]. To ensure the reusability of fibers, it is necessary to investigate the effect of sodium hydroxide concentration and soak time on regeneration performance. The effects of different lye concentrations on fiber regeneration capacity are

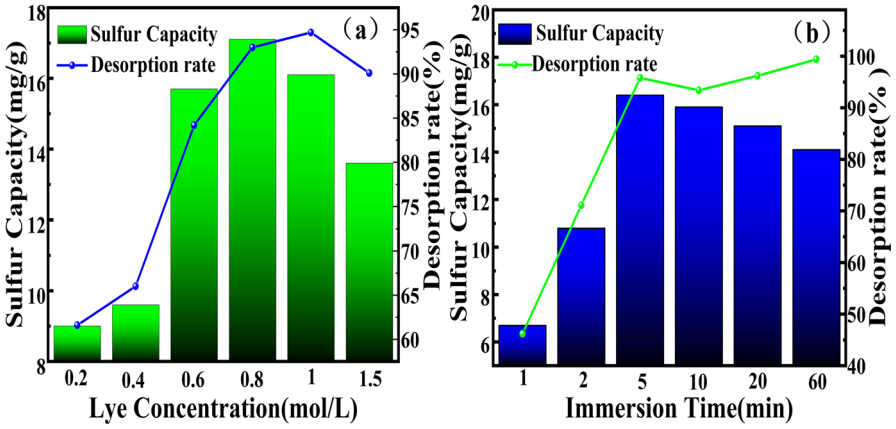

Fig.9 **a** Effect of lye concentration on fiber regeneration performance(T = 40 ℃, lye concentration = 0.8 mol/l). **b** Effect of immersion time on fiber regeneration performance (T = 40 ℃, immersion time=5 min)

shown in Fig. 9a. Similar to the trend of immersion time, the higher the lye concentration, the better the fiber regeneration per unit of time. When the lye concentration was increased to 15 mol/L, the fiber sulfur capacity showed a relatively significant decrease, which indicated that the high lye concentration had already caused damage to the fiber frame structure. In order to minimize the damage of the lye to the fiber structure, the optimal soaking lye concentration for 0.5 g saturated fiber was chosen as 0.8 mol/L. On this basis, Fig. 9b shows the effect of soaking time on fiber regeneration performance. It is not difficult to find that the desulfurization capacity of the regenerated fibers is significantly lower than that of the fresh fibers when the soaking time is less than 5 min. When the soaking time was between 5 and 20 min, the regenerated fibers regained their first desulfurization capacity, indicating that the fibers had been regenerated. As the soaking time continued to be extended, the sulfur capacity of the regenerated fibers showed a decreasing trend, indicating that the lye had eroded the fibers and caused damage to the fiber structure. In order to obtain better desulfurization performance and minimize the regeneration time, the optimal soaking time for 0.5 g saturated fiber should be 5 min. In addition, the changes in the desorption rate of H_2S on the fiber by the lye showed the same trend for different lye concentrations and soaking times. The desorption rate increased with the increase in soaking time and lye concentration. When the lye concentration reached 0.8 mol/L and the soaking time reached 5 min, the desorption rate no longer increased by increasing the concentration or extending the time, indicating that the H_2S adsorbed on the fiber had been fully eluted. In summary, we chose 0.5 g of fiber placed in 0.8 mol/L alkali soaking for about 5 min as the best regeneration operating conditions.

Effect of the number of cycles on the regeneration performance

Ten desulfurization–regeneration experiments were carried out using 0.8 mol/L sodium hydroxide solution as the desorption agent, and the results are shown in Fig. 10. The adsorption capacity of the aminated fibers gradually decreased with the increase of the number of uses, which may be due to the adsorption sites (–NH–/–NH_2 groups) on the fiber surface being shed during the use

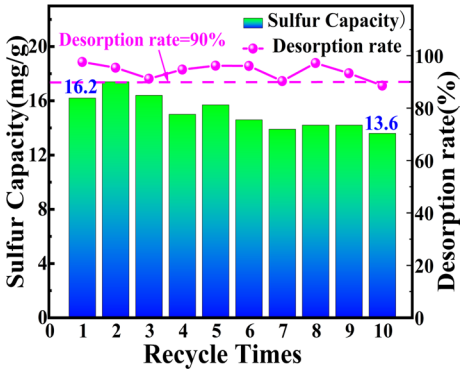

Fig.10 The reusability of $PANF_{DETA}$ for H_2S adsorption

or regeneration process[45]. It is noteworthy that after ten cycles of the adsorption–desorption process, $PANF_{DETA}$ was still able to maintain the desorption rate of H_2S at about 90%, which indicates the cause of the decrease in sulfur capacity is not due to incomplete regeneration but to the structural damage of the fiber itself. The sulfur capacity of $PANF_{DETA}$ after ten cycles of adsorption and desorption is still 13.6 mg g^{-1}, 83.9% of the initial adsorption capacity. This is unquestionably excellent. Based on the above results, we believe that $PANF_{DETA}$ has excellent regeneration performance, which is favorable for its practical application.

Mechanism

A possible mechanism of adsorption and desorption occurring on the fiber surface was proposed in conjunction with the experimental phenomena, as shown in Fig. 11. The introduction of amine groups on the fiber surface provides many bindable alkaline sites for hydrogen sulfide or sulfur hydride, which plays a crucial role in enhancing the sulfur capacity. The acid–base reaction between the two and the physical adsorption by the pore structure of the fiber itself is the fundamental reason for the ability of the fiber to adsorb H_2S. The process is chemisorption, so an appropriate increase in temperature facilitates the adsorption process. Similarly, moisture can promote the ionization of hydrogen sulfide, and the affinity between the charged sulfur hydrogen root and the amine group is more potent [46], so the presence of moisture can facilitate the adsorption reaction. The following reactions will occur in the solution during the lye immersion [47].

$$R - NH_3^+HS^- + NaOH = R - NH_2 + H_2O + NaHS \tag{3}$$

$$NaHS + NaOH = Na_2S + H_2O \tag{4}$$

$$R - NH_3^+HS^- + Na_2S = R - NH_2 + 2NaHS \tag{5}$$

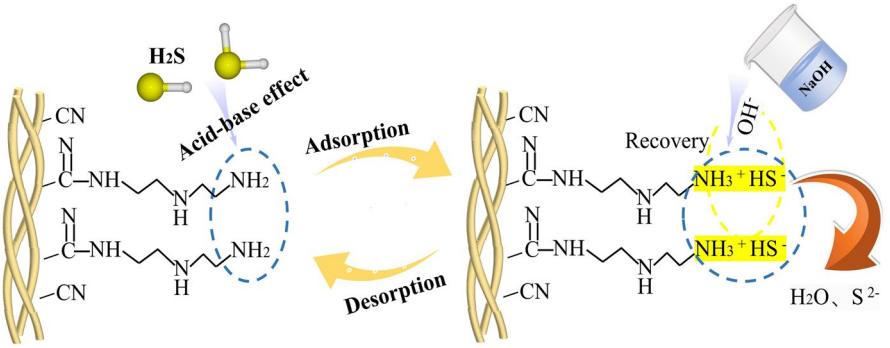

Fig.11 Possible adsorption and desorption reactions on the fiber's surface

The lye can effectively elute the HS^- immobilized on the fiber surface, and the amine group is restored to its original state to achieve regeneration.

Conclusion

In this work, aminated polyacrylonitrile was synthesized directly from commercially available polyacrylonitrile fibers to remove hydrogen sulfide from natural gas at ambient temperature. Desulfurization experiments were used to study the adsorption behavior of $PANF_{DETA}$ under different conditions on H_2S. In addition, we focused on the excellent regenerative properties of fibers as desulfurizer substrate materials to evaluate their potential as desulfurizer matrix materials. The results showed that the sulfur capacity of the aminated fiber increased by as much as 15 times compared to the pure fiber. Surprisingly, after ten cycles of continuous desulfurization–regeneration under optimal regeneration conditions, the aminated fibers still maintained 83.9% of the sulfur capacity level of the fresh sample. The alkali solution could effectively elute the adsorbed H_2S molecules from the fibers during this process. The relevant characterization results of the samples also confirm this to some extent. These results of our study suggest that polyacrylonitrile may be a suitable substrate material for desulfurizers, which will provide new ideas for removing hydrogen sulfide from natural gas at room temperatures. Based on this, our future research will focus on further enhancing the adsorption capacity.

Author contributions ZL and KQ conceived the presented idea. ZL undertook the bulk of the experiments and completed the manuscript. YW, JP, SC, and XS participated in the experiment. Sun Gang and Ma Yue helped us with our experiments outside of school. KQ supervised the findings of this work. All authors discussed the results and contributed to the final manuscript.

Funding The research was funded by China National Science and Technology Major Project (2016ZX05017) and the Sinopec Group Corporation 2020 Science and Technology Project "Organic Sulfur Catalytic Hydrolysis Technology Improves Quality Research"(No.120049–1).

Availability of data and materials All data generated or analyzed during this study are included in this published article.

Declarations

Conflict of interests The authors declare that there is no competing financial or non-financial interest that could have appeared to influence the work reported here.

References

1. K. Qiu, Z. Liu, Y. Dong, L. Liu, W. Li, S. Niu, Z. Jin, Chem Eng & Technol. **45**, 1867 (2022)
2. C. Ma, Y. Zhao, H. Chen, Y. Liu, R. Huang, J. Pan, J. Environ. Chem. Eng. **10**, 107370 (2022)
3. A. Pudi, M. Rezaei, V. Signorini, M.P. Andersson, M.G. Baschetti, S.S. Mansouri, Sep. Purif. Technol. **298**, 121448 (2022)
4. M.N. Hossain, H.C. Park, H.S. Choi, Catalysts **9**, 229 (2019)

5. F. Tian, Q. Shen, Z. Fu, Y. Wu, C. Jia, Fuel Process Technol. **128**, 176 (2014)
6. J. Warych, M. Szymanowski, Ind. Eng. Chem. Res. **40**, 2597 (2001)
7. C. Xu, J. Chen, S. Li, Q. Gu, D. Wang, C. Jiang, Y. Liu, J. Hazard. Mater. **403**, 123806 (2021)
8. S. Faramawy, T. Zaki, A.E. Sakr, J Nat Gas Sci Eng **34**, 34 (2016)
9. D. Liu, S. Chen, X. Fei, C. Huang, Y. Zhang, Ind. Eng. Chem. Res. **54**, 3556 (2015)
10. J.M. Sánchez-Hervás, M. Maroño, R. Fernández-Martínez, I. Ortiz, R. Ortiz, M.B. Gómez-Mancebo, Fuel **314**, 122724 (2022)
11. T. Xu, M. Zhang, F. Zhao, J. Zhao, W. Cong, C. Xie, J. Li, J. Hazard. Mater. **440**, 129753 (2022)
12. A. Mohammadi, Z. Saadati, S. Joohari, Environ. Prog. Sustainable Energy **38**, e13258 (2019)
13. S. Kim, B. Bajaj, C.K. Byun, S.J. Kwon, H.I. Joh, K.B. Yi, S. Lee, Appl. Surf. Sci. **320**, 218 (2014)
14. G. Coppola, D. Papurello, Clean Technol. **1**, 40 (2018)
15. S. Bai, C. Chen, R. Luo, A. Chen, D. Li, Sens. Actuators B Chem. **216**, 113 (2015)
16. L. Sigot, G. Ducom, P. Germain, Chem. Eng. J. **287**, 47 (2016)
17. Y. Belmabkhout, G. De Weireld, A. Sayari, Langmuir **25**, 13275 (2009)
18. Y. Wang, C. Yang, C. Zhang, M. Duan, H. Wang, H. Fan, J. Lin, Fuel **319**, 123845 (2022)
19. A. Georgiadis, N. Charisiou, Goula, Catalysts **10**, 521 (2020)
20. Z. Chen, X. Liu, W. Wei, H. Chen, B.J. Ni, Water Res. **221**, 118820 (2022)
21. T.C. Mokhena, K.P. Matabola, T.H. Mokhothu, A. Mtibe, M.J. Mochane, G. Ndlovu, J.E. Andrew, Sep. Purif. Technol. **288**, 120666 (2022)
22. Z. Chen, W. Wei, X. Liu, B.J. Ni, Water Res. **221**, 118846 (2022)
23. Z. Chen, R. Zheng, W. Wei, W. Wei, W. Zou, J. Li, H. Chen, Resour. Conserv. Recycl. **178**, 106037 (2022)
24. G. Zhang, H. Sheng, D. Chen, N. Li, Q. Xu, H. Li, J. Lu, Chem. Eur. J. **24**, 15019 (2018)
25. S. Yi, B. Ghanem, Y. Liu, I. Pinnau, W.J. Koros, Sci. Adv. **5**, 5459 (2019)
26. Z. Chen, J. Fang, W. Wei, H.H. Ngo, W. Guo, B.J. Ni, J Clean Prod **371**, 133676 (2022)
27. Y. Wang, Y. Liu, Z. Wang, Z. Wang, Chem. Eng. J. **434**, 134430 (2022)
28. D. Wang, Z. Wang, J. Int, Sci. **5**, 119 (2018)
29. Y. Liu, X. Xu, Y. Wei, Y. Chen, M. Gao, Z. Zhang, J. Liang, Nano Lett. **22**, 3784 (2022)
30. X.L. Shi, B. Sun, Y. Chen, Q. Hu, P. Li, P. Duan, J. Catal. **372**, 321 (2019)
31. S. Deng, R.B. Bai, Environ. Sci. Technol. **37**, 5799 (2003)
32. Y. Jung, Y.G. Ko, T. Do, Y. Chun, U.S. Choi, C.H. Kim, J. Hazard. Mater **378**, 120726 (2019)
33. W. Xu, W. Zheng, F. Wang, Q. Xiong, X.L. Shi, Y.K. Kalkhajeh, H. Gao, Chem. Eng. J. **403**, 126349 (2021)
34. S. Deng, G. Zhang, X. Wang, T. Zheng, P. Wang, Chem. Eng. J. **276**, 349 (2015)
35. K. Li, C. Wang, P. Ning, X. Sun, X. Song, Y. Wang, Res. Chem. Intermed. **46**, 3459 (2020)
36. Y.G. Ko, U.S. Choi, Sep. Purif. Technol. **57**, 338 (2007)
37. J. Zhou, M. Li, L. Zhong, F. Zhang, G. Zhang, Colloids. Surf. A Physicochem. Eng. Asp. **513**, 146 (2017)
38. C.Y. Yang, N.T. Nguyen, C.M. Ma, C.T. Chang, J. Nanosci. Nanotechnol. **16**, 1945 (2016)
39. A. Kausar, J. Plast. Film Sheet. **35**, 295 (2019)
40. C. Yang, M. Florent, G. de Falco, H. Fan, T.J. Bandosz, Chem. Eng. J. **394**, 124906 (2020)
41. Z. Liu, K. Qiu, Y. Dong, Z. Jin, L. Liu, J. Wu, Korean J Chem Eng **1000**, 1 (2022)
42. W. Zheng, Q. Wu, W. Xu, Q. Xiong, Y.K. Kalkhajeh, C. Zhang, H. Gao, Environ. Sci.: Water Res. Technol. **8**, 607 (2022)
43. R. Saeedirad, S. Taghvaei Ganjali, M. Bazmi, A. Rashidi, J. Taiwan Inst Chem Eng **82**, 10 (2018)
44. X. Xu, X. Cao, L. Zhao, T. Sun, Chemosphere **111**, 296 (2014)
45. W. Li, R. Chen, Q. Liu, J. Liu, J. Yu, H. Zhang, J. Wang, J. ACS Sustain. Chem. Eng. **6**, 13385 (2018)
46. J. Xiao, G. Xu, L. Wang, P. Li, W. Zhang, N. Ma, M. Tao, J Ind. Eng Chem. **77**, 65 (2019)
47. S.K. Nataraj, K.S. Yang, T. Aminabhavi, Prog. Polym. Sci. **37**, 487 (2012)